Fizika Nizkikh Temperatur, 2003, v. 29, No. 3, p. 237–249

Coherent motion and anomalous transport properties of exciton and hole polarons with intrinsic vibrational structure

A.M. Ratner

B. Verkin Institute for Low Temperature Physics and Engineering of the National Academy of Science of Ukraine, 47 Lenin Ave., Kharkov, 61103, Ukraine
E-mail: Ratner@ilt.kharkov.ua

Received June 25, 2002

It is shown that intrinsic vibrational degrees of freedom, inherent in two-atom exciton and hole polarons, drastically affect their transport properties in wide-band dielectrics (rare-gas solids and alkali halides). A fast excitonic energy transport and a comparatively high hole mobility, experimentally observed and attributed to two-site polarons tightly bound with the lattice, cannot be explained by the conventional theory of small-radius polarons that predicts their negligibly weak diffusion, exponentially small in the ratio of the binding energy to temperature. The theory, developed below with allowance for the intrinsic vibrational structure of two-site polarons describes qualitatively a large relevant set of experimental data which seem anomalous from the viewpoint of the conventional theory.

PACS: **71.38.+i**

Introduction

In dielectrics with broad exciton and hole bands, formed by a strong exchange interaction, the most stable excitonic and hole states are known to be of a two-site type (two neighboring atoms, strongly brought together, form a quasi-molecule with the exchange binding growing sharply with a decrease of the interatomic distance). Such two-atom electronic excitations with an intrinsic vibrational degree of freedom are inherent and distinctly observed in the electronic spectra of rare-gas solids [1] and alkali-halide crystals [2] (these classes of dielectrics have common features of electronic structure, outlined at the beginning of Sec. 1).

Such two-atom excitations are usually treated as polaronic states tightly bound with the lattice. In the theory of polarons, the energy of this binding is identified with the separation Δ of the polaron level from the bottom of the corresponding band. For the classes of dielectrics mentioned, the separation Δ is of the scale of 1eV.

However, the transport properties of such two-site excitations cannot be satisfactorily described within the conventional polaronic theory [3–6]. For a strongly bound polaron, the latter predicts an exponentially small diffusion coefficient

$$D = D_0 \exp(-U_{\text{act}}/T_{\text{eff}}), \qquad (1)$$

where the activation energy U_{act} is close to Δ and T_{eff} stands for an effective temperature (expressed in energy units) which at low temperatures makes allowance for the lattice zero-vibration energy. This inference of the theory drastically contradicts experimental evidence (analyzed in Secs. 5 and 6) of a fast transport of charge and especially energy by two-site polarons.

The physical reason of such discrepancy consists in the following. The conventional theory considers the hopping of a polaron devoid of intrinsic structure. Such a polaron, staying near the lattice site A, causes lattice deformation around it and a corresponding lowering of the polaron level by an amount $\Delta \approx U_{\text{act}}$. The electron or hole, localized at the site A at a deep level E_A, can go over to a neighboring site B only under a fluctuation of its lattice surroundings strong enough to lower the level of the electronic state, localized at the site B, down to E_A. The energy of such a lattice deformation is found to be close to Δ which is

described by Eq. (1). Such a simple notion is not applicable to a two-site polaron: its intrinsic degree of freedom enables it to move continuously together with the deformation cloud maintaining the polaronic state. In other words, the lattice deformation around a new position of a two-site polaron is mainly produced not by thermodynamic fluctuations but by the continuous motion of the polaron itself.

In the present paper, the theory of the continuous motion and transport properties of two-site polarons is developed and qualitatively compared with experiment as applied to rare-gas and alkali-halide crystals. First, in Sec. 1, it is shown that a fast transport in these dielectrics is conditioned by some features of their electronic spectrum, viz., the exchange nature of the exciton and hole bands and their anisotropic structure, entailing one-dimensional translational motion. As a result, the energy barrier, impeding the translational motion, is sharply diminished as compared to a structureless polaron with the same binding energy Δ.

In the next Sections, 2, 3, and 4, such one-dimensional motion of two-site excitations is explored, depending on the main factors, dictating their character, viz., the vibrational energy of a two-atom quasi-molecule and the height of the «residual» energy barrier. In the case of a high vibrational energy, much exceeding the barrier height and temperature, the translational motion has a coherent directional character (Sec. 3), but under thermodynamic equilibrium (Sec. 4), the translational motion gains diffusive character and transport is slowed down by several orders of magnitude compared to the former case. In Secs. 5 and 6 a qualitative comparison with experiment is carried out as applied to these two cases.

1. Continuous one-dimensional motion of polarons with intrinsic degrees of freedom

This manner of translational motion is to a large degree conditioned by a feature of the electronic spectrum of rare-gas or alkali-halide crystals. In the case of a rare-gas crystal, the system of excitonic bands occupies the upper part of the dielectric gap (more than 10 eV wide) and originates from the Rydberg atomic excited states $ns^2np^5(n+1)s$. A significant bandwidth of about 1 eV is due to a rather strong exchange interaction between an excited atom and adjacent ground-state ones. On the other hand, this strong exchange results in the existence of two-site excitonic states. A two-site exciton is formed on adjacent atoms which are brought together, providing a much stronger attractive exchange interaction compared to regular lattice sites. Such a two-atom quasi-molecule with a bond energy of about 1 eV is quite similar (judging from spectroscopic data) to the corresponding excimer molecule in the gas phase [1]. In a crystal, the vibrational levels of such a quasi-molecule turn to narrow subbands practically covering the energy extent of all excitonic bands [7,8].

The dispersion law of excitons or holes is determined by the interatomic overlap of excited states $ns^2np^5(n+1)s$, which mainly coincides with the overlap of the np-hole states ns^2np^5 centered at adjacent sites. This overlap is largest in the direction of the p-state axis and gives rise to a sharply anisotropic excitonic dispersion law [9]. Actually, a free exciton or hole moves in the direction of the minimal effective mass, which coincides with the axis of the np-hole and dictates the axis direction of a two-site exciton or hole polaron.

The outlined picture qualitatively holds for alkali halide crystals with large anions and small cations (e.g., NaI, NaCl, and KI). The exciton and hole states (free or self-trapped), formed in the sublattice of closed-shell anions, are similar to those of rare-gas solids. These electronic excitations, associated with the anion sublattice, cannot be noticeably interfered by small cations with a very high ionization potential.

The translational motion of two-site excitons and holes is described by the same equations and has the same qualitative features (a distinction in their behavior, caused by essentially different lifetimes, will be considered in Secs. 3 and 4). So far this distinction does not manifest itself, we will speak; for definiteness, about holes.

Let us trace qualitative features of the motion of a two-site self-trapped hole (called also two-atom ionized quasi-molecule) in a rare-gas crystal. The molecular ion consists of two identical rare-gas atoms A and B with a common shared px-hole in their outer shell (the x-axis coincides with the axis of the atomic P state). These atoms are brought together by a strong exchange interaction conditioned by the hole. The exchange potential, mainly proportional to the overlap of the px-states centered at the points A and B, strongly diminishes with an increase of the angle between the x axis and the direction AB [9]. So, the hole, forming the quasi-molecule AB, is polarized in the direction x coincident with the quasi-molecule axis AB. The translational motion of the hole is conditioned by the exchange interaction between the atoms A, B and other atoms. Since this exchange is significant only for adjacent atoms lying in the same axis x, the motion of a two-site hole is of one-dimensional character (which is evidenced experimentally; see Sec. 6, Item 2). Below we will consider the motion of such hole along the atomic chain, allowance being made for its static three-dimensional surroundings. The same relates to two-site excitons as well.

The nontrivial phenomena under consideration are conditioned by a non-pair exchange interaction of atoms among which a hole is distributed [9,10]. Such an exchange is described by an usual exchange Hamiltonian

$$\mathcal{H} = \sum_{n=1}^{N} E_0 a_n^+ a_n - \\ -\sum_{n=1}^{N-1} V(x_{n+1} - x_n)(a_n^+ a_{n+1} + a_n a_{n+1}^+). \qquad (2)$$

Here E_0 is the site hole level, a_n^+ is the creation operator for a hole on the nth atom, $-V(x)$ is the negative exchange energy strongly dependent on the interatomic distance x, and x_n is the coordinate of the nth atom counted along the chain. The hole is generally distributed among several atoms, as described by the eigenfunction of the Hamiltonian (2)

$$\Psi = \sum_n c_n \varphi_n, \qquad \sum_n |c_n|^2 = 1, \qquad (3)$$

where $|c_n|^2$ is the portion of the hole at the nth site, and

$$\varphi_n = a_n^+ \Psi_{\text{ground}} \qquad (4)$$

is the corresponding site state of the crystal (Ψ_{ground} is its ground state).

The same Hamiltonian (2) also describes an exciton, with the sole difference that the operator a_n^+ in Eqs. (2), (4) creates an atomic excitation instead a hole at the nth site. Therefore, all of the inferences, drawn below in this Section and in Sec. 2, are related to holes and excitons to the same degree.

The lowest eigenvalue of the Hamiltonian (2) for arbitrary fixed positions of the atoms is

$$W = E_0 - \max\left\{\sum_n V(x_{n+1} - x_n) c_n c_{n+1}\right\}, \sum_n |c_n|^2 = 1 \qquad (5)$$

(energy is minimized with respect to the set $\{c_n\}$). If the occupation numbers c_n were fixed, the quantity (5) as a function of atomic coordinates would be the sum of pair potentials $V(x_{n+1} - x_n)$ multiplied by fixed coefficients. But in fact the occupation numbers c_n depend substantially on $V(x_{n+1} - x_n)$ and, hence, on x_n; therefore, the hole energy (5) cannot be reduced to the sum of pair potentials. This circumstance is of fundamental importance: it results in a substantial lowering of the energy barrier that impedes translational motion (within the approach of pair potential, this barrier is found to be much higher and the translational motion much slower [7,8]).

For a periodic chain, consisting of N atoms, the minimum of energy (5) is achieved at $c_n = N^{-1/2}$, which corresponds to the lowest band state.

We consider the opposite case of a tightly bound polaronic state with a hole localized near two adjacent atoms brought together (they are numbered, for definiteness, by indices n = 2 and 3). For this pair of atoms, the exchange multiplier $V(x_3 - x_2)$ in (5) strongly exceeds the rest of multipliers $V(x_{n+1} - x_n)$; hence, the energy (5) is minimized at $c_2 = c_3 \approx 2^{-1/2}$, the rest of the coefficients c_n being much less. Such a state labeled by A is shown in Fig. 1, where the areas of the circles denote the portion of the hole, $|c_n|^2$, localized on atoms. Let us trace the change from the state A to a similar state D with the hole, shifted by one chain period, first keeping to the traditional notion and then with allowance for the nonpair exchange interaction.

Within the traditional notion [3–6], the state A turns immediately to the state D: the hole hops by one lattice period from the atomic pair (2,3) to the pair (3,4). To make such a hop possible, an adjacent atom 4 (devoid of a hole until the hop occurs) must be moved towards atom 3 strongly enough to reduce the distance (4,3) down to the distance (3,2). The energy of such a deformation nears the binding energy, so that the hopping rate is described by Eq. (1).

If the nonpair exchange interaction is taken into account, the picture becomes quite different: the initial state A turns to the final state D through a continuous sequence of intermediate states (B, C...) in the following way. To minimize energy (5), atom 4, when

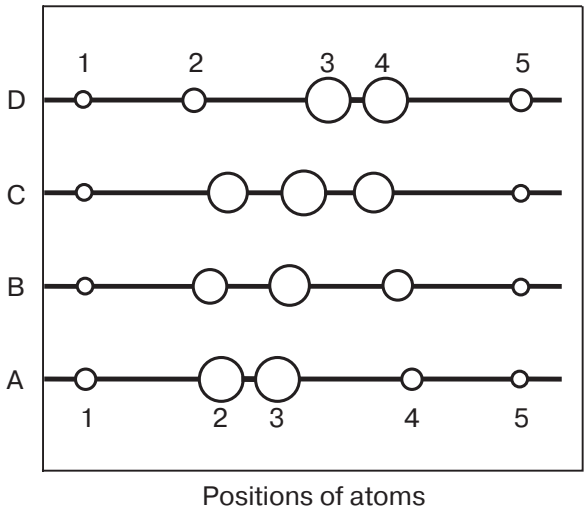

Fig. 1. Translational motion of a two-site self-trapped hole via its continuous redistribution among atoms shown by circles (the areas of the circles indicate the portion of the hole on the atoms). The hole sequentially passes the states A, B, C, D without overcoming a significant barrier. This scheme relates to a two-site exciton as well.

moving towards the pair (2,3), gets a portion of hole that increases with decreasing separation (4,3) (as shown by the varying areas of the circles). Thus, the distribution of the hole among atoms follows their motion continuously (not by a jump as within the conventional scheme). This sharply diminishes the energy barrier B to be overcome when changing from the initial state A to the final state D.

Nevertheless, the height of the «residual» energy barrier essentially influences the translational motion of a two-site hole that, in view of its long lifetime, moves in thermodynamic equilibrium with the lattice and occupies rather low vibrational levels comparable with the barrier height. Unlike a hole, a two-site exciton, during its short lifetime, comparable with the time of vibrational relaxation, occupies high vibrational levels. As long as the vibrational energy much exceeds the barrier height, a two-site exciton moves in a coherent directional way practically irrespective of the barrier.

For this reason, the barrier is of great importance only for the motion of holes. In the next Section, the barrier is investigated as applied to two-site holes, but the obtained results are related to two-site excitons as well.

2. Energy barrier for translational motion

To obtain the barrier, let us introduce the total adiabatic potential of an N-atom chain containing one hole:

$$W_{\text{tot}}(x_1,\ldots,x_N) = W(x_1,\ldots,x_N) + \\ + \sum_{n=1}^{N-1} u_0(x_{n+1} - x_n) + \sum_{n=1}^{N}\sum_{\mathbf{R}} u_0(|\mathbf{r}_n - \mathbf{R}|). \quad (6)$$

The total potential consists of the hole energy (5) (first term on the right-hand side of Eq. (6)) and the sum of the pairwise ground-state interatomic potentials u_0 taken along the chain (second term) as well as between every chain atom (with coordinates $\mathbf{r}_n$) and the immovable lattice atoms not belonging to the chain (with coordinates $\mathbf{R}$). To find the barrier, one has to continuously change from the state A to the state D (see Fig. 1) via reducing the distance (4,3), the rest of interatomic distances being adjusted to the minimum of the total potential (6) at a given separation (4,3). Such a trajectory in the space $(x_1,\ldots, x_N)$ inevitably passes a symmetric configuration C (Fig. 1) that provides an extremum of W_{tot}. Usually a two-site hole state A or D is assumed to be stable, that is

$$W_{\text{tot}}(\text{C}) > W_{\text{tot}}(\text{A}). \quad (7)$$

If the condition (7) is met, the barrier height should be defined as

$$B = W_{\text{tot}}(\text{C}) - W_{\text{tot}}(\text{A}) = W_{\text{tot}}(\text{C}) - W_{\text{tot}}(\text{D}). \quad (8)$$

Below, the barrier definition (8) will be used without restriction (7), a negative B being understood in the meaning of the energy separation between the stable three-atom state C and unstable two-atom state A or D.

To calculate the barrier (8) for a real crystal, it is necessary to reconstruct the total potential (6). It contains, besides the ground-state potential u_0 which is known to good accuracy [9], the resonance contribution (5) defined through the exchange potential $V(x)$, mainly proportional to the interatomic overlap integral $J(x)$ (x is interatomic distance). The dependence $J = J(x)$ can be approximately derived from the ground-state repulsion potential that, on one hand, is in main proportional to $J(x)^2$ and, on the other hand, is known to decrease with increasing x nearly as $\exp(-12x/l)$ (l is the interatomic distance in the ideal lattice) [9]. Thus, the exchange potential V can be approximated in the form

$$V(x) = V_0 \exp\left\{q\frac{l-x}{l} + \gamma\left(\frac{l-x}{l}\right)^2\right\},\ q \approx 6. \quad (9)$$

Here a small quadric term, influencing the barrier, is allowed for. The preexponential V_0 (close to 0.24 eV for solid krypton) can be derived from the width of the hole band formed in the ideal lattice ($V = V_0$ at $x = l$).

Below, the parameters q, γ and $V_0 = 0.24$ eV are taken for solid krypton. For hole states, there are no spectroscopic data to derive the exchange interaction parameters q and γ. But q and γ can be derived for the lowest two-site excitonic state via fitting the corresponding luminescence spectrum (energy position and halfwidth) with experiment. Note that the exchange interaction, resulting from a p-hole in the valence shell, cannot noticeably differ for the hole and exciton: the p-electron is completely removed in the former case or carried over to a large-radius Rydberg state in the latter. Making use of this, let us fit the required parameters q and γ with the two-site exciton luminescence band of solid krypton. The fitting can be carried out with nearly the same accuracy with q varying in the range 6 ± 0.5 and the corresponding values of γ given in Table 1 as a function of q.

For every set (q, γ), Table 1 presents the barrier (8) calculated with the exchange potential (9) for two lattice parameters 0.5812 and 0.5850 nm related to the temperature of 80 and 110 K, respectively [11]. (Note that the lattice parameter, appearing in the last term of Eq. (6), essentially influences the barrier: it grows with a decrease of the distance between chain atoms and the nearest lattice atoms lying beyond the chain.)

Table 1

Barrier height (8) for solid krypton calculated using the exchange potential (9) with different q and γ for lattice periods 0.5812 and 0.5850 nm related to the temperature 80 and 110 K, respectively

q	γ	B, K	
		T=80 K	T=110 K
5.66	0.07	473	410
5.76	0.06	386	308
5.865	0.05	288	196
5.97	0.04	168	60
6.08	0.03	38	–84
6.22	0.02	–62	–199
6.36	0.01	–192	–343
6.51	0	–335	–500

Table 1 demonstrates a high sensitivity of the barrier to the exchange potential parameters as well as to the lattice period (its thermal increase by 0.7 % lowers the barrier by about 100 K). The point is that the potential (6), whose maximum makes up the barrier, is formed by the sum of positive and negative quantities with a scale of 1 eV, which exceeds the characteristic height of the barrier by about two orders of magnitude. A slight variation of a separate summand causes a significant relative variation of the barrier.

As will be shown below, the barrier height influences the hole motion in an essential and nontrivial way (the specific way of realizing the barrier is of much less importance).

Song [12] has estimated the barrier B for a two-site hole quasi-molecule in solid argon within the approximation of pair potentials. The interaction between the atoms of the quasi-molecule (atoms 2, 3 in Fig. 1, state A) and between every atom of the quasi-molecule and an adjacent atom not belonging to it (the pairs 1,2 and 3,4) was described by the same potential that was assumed to be independent of the hole distribution between these atoms. As a result, it was found that the barrier height does not exceed 0.05 eV = = 600 K, which agrees in order of magnitude with Table 1.

3. Directional translational motion of a two-site polaron (exciton) on high vibration levels

Due to its short lifetime, comparable with the vibrational relaxation time, a two-site exciton dwells on high vibrational levels during a significant part of its existence. The directional translational motion, possible only on high vibrational levels, manifests itself in an anomalously fast energy transport.

Even within the one-dimensional model (grounded in Sec. 1), the rigorous quantum-mechanical description of such a complicated phenomenon seems unrealistic. Below, only the electronic subsystem will be considered in a quantum-mechanical way; the lattice motion will be described classically in the adiabatic approximation. The latter is justified since the separation between the lowest level of the Hamiltonian (2) and the rest of its levels much exceeds both T and the vibrational frequencies of the chain (expressed in energy units). Within this model, the lattice is represented by an N-atom chain (its length is chosen large enough that the calculation results are independent of N). The rest of the lattice atoms are assumed to be placed strictly at their sites and are taken into account by the last term in the total potential (6).

Keeping to the adiabatic scheme within the one-dimensional model, let us first consider the lowest excitonic state formed at arbitrary fixed positions of N atoms. The energy of this state W is given by Eq. (5). According to a standard procedure, the partial derivatives of the right-hand side of Eq. (5), added to the sum $W\Sigma c_n^2$, should be taken with respect to the coefficients c_n and equated to zero. This results in the system of linear homogeneous equations

$$\begin{aligned} &V(x_2 - x_1)c_2 - Wc_1 = 0, \\ &V(x_{n+1} - x_n)c_{n+1} + V(x_n - x_{n-1})c_{n-1} - Wc_1 = 0 \quad (1 < n < N), \\ &V(x_N - x_{N-1})c_{N-1} - Wc_N = 0. \end{aligned} \tag{10}$$

Let D be the N-order determinant of this equation system. The excitonic energy $W(x_1,\ldots,x_N)$ at arbitrary fixed positions, $x_1, \ldots, x_n$, of the chain atoms can be obtained from the equation

$$D(W, x_1,\ldots, x_N) = 0 . \tag{11}$$

Of N roots of this determinant, the lowest one corresponds to the self-trapped excitonic state and is separated by a large gap from all the other roots, which belong to a slightly distorted excitonic band. The least root is identified with W. Substituting W into (6),

we obtain the total adiabatic potential W_{tot} of the N-atom system with a self-trapped exciton.

The classical motion of the system of N atoms with the non-pair potential (6) is described by the equation

$$M_0 \frac{d^2 x_n}{dt^2} + \frac{\partial W_{tot}(x_1,\ldots,x_N)}{\partial x_n} = 0 \qquad (12)$$

with the atom mass M_0.

Equation (12) was solved numerically for solid krypton under the following conditions. At the initial time $t = 0$, a two-site quasi-molecule with the vibrational energy E_{vib} arose on two adjacent atoms arbitrarily chosen inside the atomic chain. In the course of motion, the electronic excitation is distributed among 4 atoms (as shown in Fig. 1). The nonequilibrium vibrational energy, concentrated within this four-atom complex, is maintained at the given level E_{vib} via a weak continuous input of energy. The rest of atoms are in equilibrium with the lattice at a given constant temperature T. In the course of motion, the total average kinetic energy of all atoms of the chain (except the above four-atom complex) was maintained at the level $(N–4)T/2$ via a very slow injection or carrying away of heat. Simultaneously the dispersion of this kinetic energy as a function of time was maintained at a proper level of $(N–4)^{1/2}T/2$ (to that end, every atom of the chain received weak random augmentations to its momentum with the frequency of lattice vibrations).

The computer solution of Eqs. (11),(12) exhibits some general features. The strongest resonance bond, formed between two atoms with the numbers L and L+1, comprises more than half the electronic excitation (this means that $c_L^2 + c_{L+1}^2 > 0.5$); on four atoms (L–1, L, L+1, L+2) the excitation is concentrated practically completely. The vibrational energy of this four-atom complex decreases slowly (by about 1 % per period) in the course of thermal relaxation. Note that in the corresponding quantum-mechanical system the vibrational relaxation occurs substantially (by two orders of magnitude) more slowly in view of the relevant conservation laws and complicated phase relations between different vibrational wave functions [9]. This circumstance was taken into account by a weak steady input of energy into the four-atom complex, which maintained its vibrational energy at the initial level.

The character of the motion is determined by the parameters E_{vib} and T. Numerical analysis of the Eqs. (11),(12) shows that the translational motion of the four-atom complex can occur either in a diffusive way (through random translational shifts, one of which is shown in Fig. 1) or in a coherent directional way (through sequential shifts agreed in phase with one another). The directional motion takes place at a high vibrational energy E_{vib} and a low temperature; in the opposite case, the self-trapped exciton moves in a random diffusive way. The picture is practically independent of the barrier height B as long as $B << E_{vib}$.The boundary between these types of motion in the E_{vib}- versus-T plane is shown in Fig. 2.

Figure 3 shows the motion of the exciton center of weight

$$x_c = \sum_{n=1}^{N} |c_n|^2 x_n \qquad \left(\sum_{n=1}^{N} |c_n|^2 = 1\right) \qquad (13)$$

at different points of the E_{vib}- versus-T plane. The figure demonstrates that the motion of a two-site exciton changes its character in a similar way with increasing vibrational energy at a constant temperature (Fig. 3,*a*) or with decreasing temperature at a constant vibrational energy (Fig. 3,*b*). The directional motion of an exciton is quite stable at the right-hand side from the boundary indicated in Fig. 2, whereas at the left-hand side directional motion can be realized during short time intervals in a random way due to fluctuations.

At any temperature, the stability of the coherent translational motion of the self-trapped exciton depends strongly on its vibrational energy. This seems quite natural since this translational motion is coupled with the vibrations of the four-atom complex.

The directional motion velocity, $V = dx_c/dt$, is found to be of the scale of the sound velocity in the crystal. This is easy to understand: a longitudinal elas-

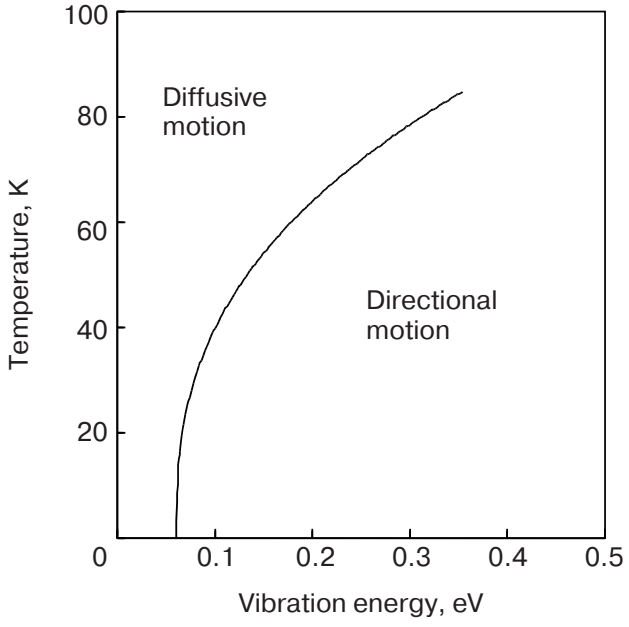

Fig. 2. Regions of the diffusive and directional motion of a two-site exciton in the plane temperature versus vibrational energy.

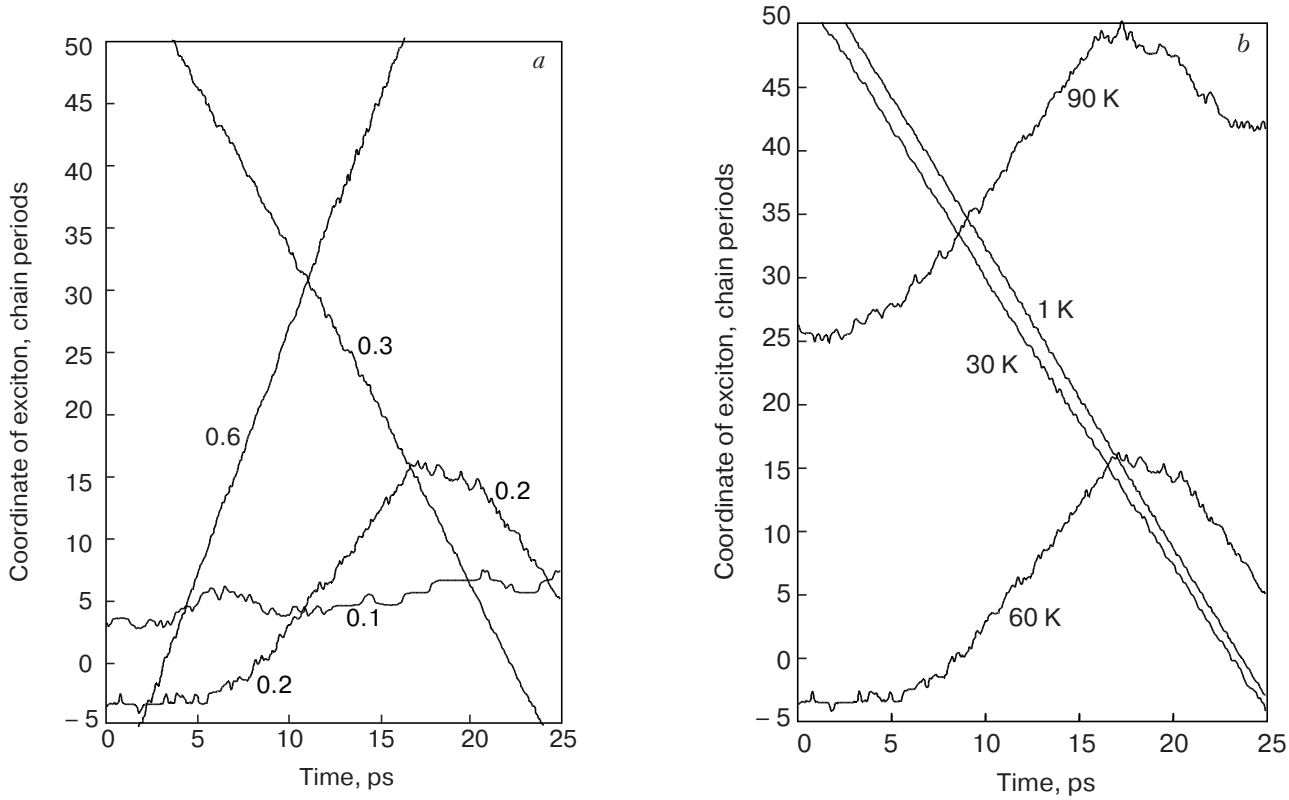

Fig. 3. Typical fragments of the motion of the exciton center of weight calculated by solving Eqs. (11), (12). The exciton coordinate in units of the chain period (ordinate axis) and time (abscissa axis) are counted from an arbitrary origin. The figure shows how the character of motion changes: (*a*) – with increasing vibrational energy (indicated in the figure in eV) at a constant temperature equal to 60 K; (*b*) – with decreasing temperature (indicated in the figure) at a constant vibrational energy equal to 0.2 eV. The directional motion is quite stable on the right of the boundary presented in Fig. 2 and arises in a random fluctuation way on the left of the boundary.

tic wave, coupled with electronic excitation, propagates in the crystal mainly in the same way as ordinary sound. As can be seen from Fig. 3,*a*, V grows with E_{vib}. The directional motion velocity was found to be proportional to $E_{\text{vib}}^{1/2}$ and practically independent of temperature and barrier height (at $E_{\text{vib}} = 0.63$ eV, V coincides with the longitudinal sound velocity in solid krypton, equal to $1.37 \cdot 10^5$ cm/s).

4. Diffusive motion of two-site polaron (hole) in thermodynamic equilibrium with lattice

Unlike short-lived excitons (with lifetime of about 1 ns), two-site hole polarons during measurement of their mobility have a long lifetime (more than 1 μs) [13], exceeding the vibrational relaxation time by 3 or 4 orders of magnitude. Therefore, a self-trapped hole moves under conditions of thermodynamic equilibrium with the lattice. Such motion was investigated by solving Eqs. (11),(12) in a way described in Sec. 3, but without the input of energy into the four-atom complex to maintain its vibrational energy at a given level. Under such conditions the hole polaron motion is of a random diffusive character, so that the hole mobility μ is connected with the hole diffusion coefficient D by the known Einstein relation

$$\mu = \frac{De}{T} = \frac{e}{2Tt} \sum_{t_j \le t} (\Delta x_j)^2, \qquad (14)$$

where e is the electron charge, T is temperature in energy units, Δx_j stands for the random shift of the center of weight of the hole at the time moment t_j; the summation extends over all statistically independent shifts occurring during time t.

To evaluate the diffusion coefficient D with sufficient accuracy, the diffusional motion of a hole was traced for a long enough time of about 5 ns; during this time, about 700 squared chain periods are accumulated in the sum (14) [11].

Unlike an exciton occupying a high vibrational level, the equilibrium motion of a self-trapped hole essentially changes its character depending on the barrier height B, as is demonstrated in Fig. 4. As can be seen from the figure, for a high barrier $B = 386$ K = $= 4.8\,T$ (upper curve in Fig. 4), a hole participates in the motion of two sharply different types: high-fre-

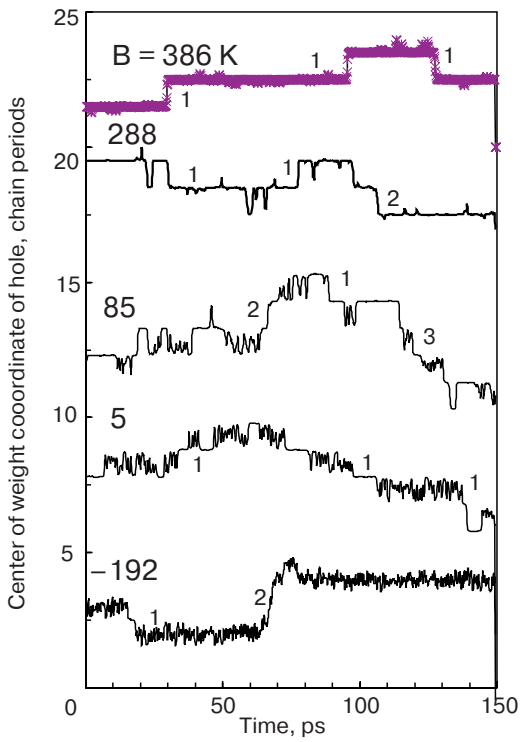

Fig. 4. Typical fragments of the diffusional motion of the center of weight of a hole in thermodynamic equilibrium with the lattice at T = 80 K, calculated for different barriers (whose height is indicated in Kelvins by the large numerals). Random translational shifts (hole «hops») are marked by small numerals indicating the hopping distance in units of the chain period. As the barrier B is lowered in the region $B < T$, the vibrational motion of the hole develops at the expense of its translational motion (therefore, as can be seen from Fig. 5, diffusion is not monotonously enhanced as the barrier is lowered).

quency vibrations with a small amplitude (merged into a thick line on the reduced scale of the figure) and random translational shifts by one chain period, which look like hops on the scale used. Note that in fact such «hops» occur in a continuous way, as shown in Fig. 1. For a lower barrier, «hops» by several (M = = 2, 3...) chain periods become possible (the meaning of such «multiple hops» will be explained below). In Fig. 4, every «hop» is marked by the number M indicating the distance of hopping in units of the chain period or, more briefly, the hopping multiplicity.

As the barrier lowers, the distinction between translational shifts («hops») of the hole and its vibrational motion is blurred. Along with usual high-frequency vibrations, low-frequency ones appear with amplitudes enhanced up to the chain period l. Such low-frequency vibrations can result (but not inevitably) in a translational shift according to the scheme of Fig. 1; their large period (up to 10 ps) corresponds to a small variation of the adiabatic potential W_{tot} when changing between the states B and C near the top of a low barrier.

It is easy to understand why the vibrational motion is well pronounced only in the case of a low barrier. Of interest are vibrations of a few atoms (the atoms 2, 3, 4 in Fig. 1) among which the hole is distributed. Such vibrations are accompanied by overcoming the barrier in both directions. For a high barrier ($B >> T$), a noticeable motion of the hole is made possible by a strong short-lived thermodynamic fluctuation during which the system has enough time to pass the barrier only in one direction; such motion looks like a series of random independent hops (quite distinct at B = = 386 K = 4.8 T). As the barrier is lowered somewhat (B = 288 K = 3.6 T), the fluctuation lifetime becomes sufficient to pass the barrier one time sequentially in both directions, which results in single-period vibrations with an amplitude near the chain period; such vibrations do not contribute to the mobility (14). When the barrier decreases and disappears (B = 85 and 5 K), the vibrational motion of the hole becomes most developed and occurs in the form of a long sequence of aperiodic oscillations interrupted by comparatively infrequent «hops». In the absence of the barrier, the vibrational motion predominates over hopping; this is the reason why the mobility at a given T achieves its maximum value not in the absence of the barrier but at $B \approx 1.5\ T$ (see Figs. 5, 6).

In order to compare the theory with experiment [13], performed for solid krypton in the interval 80 K $< T <$ 110 K, computer calculations of the mobility with the use of Eqs. (11),(12) were carried out for solid krypton at the temperatures T = 80 and 110 K (the analysis of these results, made below, permits one to extend their temperature range). For these fixed values of temperature, Fig. 5 presents the mobility μ (in units of $\text{cm}^2 \cdot \text{s}^{-1} \cdot \text{V}^{-1}$) as a function of barrier height B. It should be recalled (see Sec. 2) that B varies noticeably with temperature due to thermal expansion. In Fig. 5, this is allowed for by two scales of barrier, related to 80 and 110 K. Nearly the same results (but with a large statistic straggling) were obtained via direct calculation of the mobility with the use of Eq. (12) complemented by an electrostatic term describing the hole charge in a weak external electric field.

Along with this, it is interesting to trace how mobility depends on B/T irrespective of the way of varying the barrier (by varying the interatomic potentials or the lattice period). To that end, Fig. 6 presents the same results as in Fig. 5 in the coordinate μ versus reduced variable $B(T)/T$ for T = 80 K and 110 K. As can be seen from Fig. 6, in the region $B > T$, where the «hopping» has an activational character, the mobility

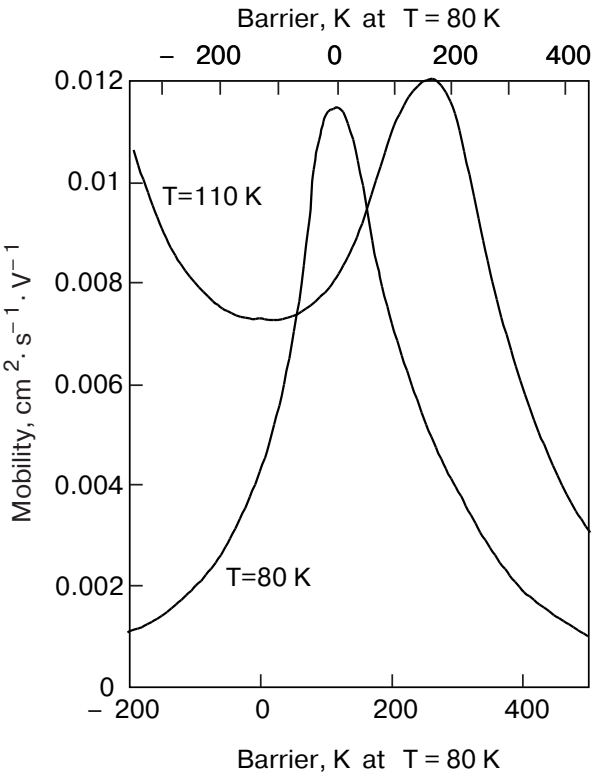

Fig. 5. Two-site hole mobility calculated for solid krypton as a function of the barrier height B at T = 80 and 110 K (B varies noticeably with temperature due to thermal expansion, which is allowed for by two scales of barrier, related to 80 and 110 K).

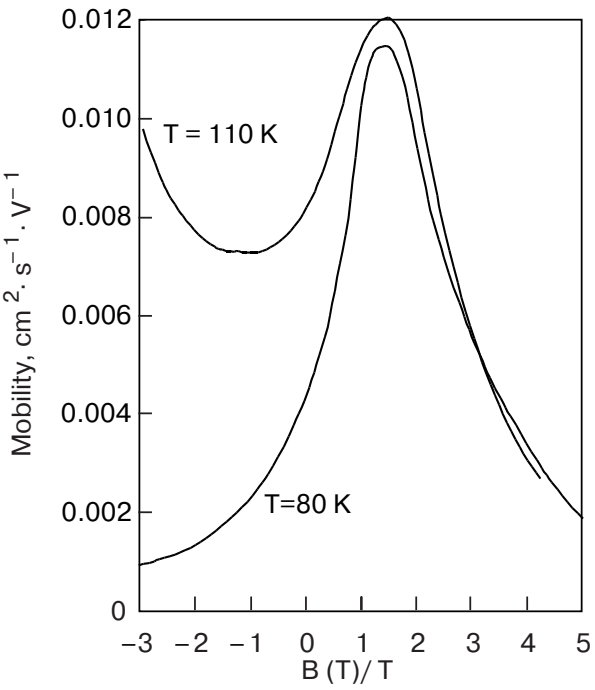

Fig. 6. The same results as in Fig. 3 presented versus the reduced variable $B(T)/T$ for T = 80 and 110 K. Note that in the region $B > T$, where the «hopping» has an activation character, mobility actually depends only on the reduced variable B/T.

actually depends only on the reduced variable B/T. Thus, the part of the curve to the right of the maximum gives the temperature dependence of the mobility in the range of lower temperatures for a positive barrier.

The absolute values of the mobility, presented in Fig. 5, agree in order of magnitude with experiment [13] (see Sec. 6) but are systematically underestimated by almost a factor of four in comparison with the experimental data. The physical reason for this quantitative discrepancy, to all appearance, is connected with underestimation of the multiple hopping of self-trapped holes.

As was shown in Sec. 3, a two-site polaron on a high vibrational level simultaneously with vibrational motion participates in the directional translational motion which is realized through sequential shifts correlated in phase. A short-time motion of such type can occur also under conditions of thermodynamic equilibrium with the lattice when a strong fluctuation brings the vibrational energy of the four-atom complex (on average equal to $4T$) to a critical level necessary for the directional translational motion. Such fluctuation enhancement of E_{vib} gives rise to a short-lived coherent elastic wave coupled with the hole. To all appearance, the model of one-dimensional chain underestimates the lifetime of such a fluctuational elastic wave. Indeed, the lattice atoms, not belonging to the chain but adjacent to it, are assumed to be immovable, whereas in fact they are involved in this elastic wave, thus enhancing the total mass of the atoms involved and the stability of the wave. The underestimation of the hopping multiplicity within the one-dimensional model entails a corresponding underestimation of the mobility (quadric in the multiplicity). This seems to be a reason for the above mentioned quantitative discrepancy between the theory and experiment.

Let us consider multiple hops in more detail and introduce the hopping multiplicity M, equal to the total length of a hop in units of chain periods. As can be seen from Fig. 4, where all hops are marked by numbers indicating their length M, multiple hops with M = 2 or 3 occur comparatively often. Hops with greater M (up to 10) occur more seldom but they noticeably contribute to the hole mobility (14). If the number of M-fold hops is denoted by ν_M, their contribution to mobility is proportional to $w_M = \nu_M M^2$. The mean multiplicity of hopping should be defined via averaging M over hops with the weights w_M:

$$\langle M \rangle = \frac{\sum\limits_M w_M M}{\sum\limits_M w_M} = \frac{\sum\limits_M \nu_M M^3}{\sum\limits_M \nu_M M^2}. \qquad (15)$$

The mean multiplicity of hopping, calculated according to (15), is shown in Fig. 7 for two temperatures as a function of $B(T)/T$. Note that multiple hopping, due to its fluctuational nature, is rapidly enhanced with increasing temperature.

5. Qualitative comparison with experiment. Energy transport by two-site excitons

Let us, first, adduce the available spectroscopic evidence for a predominant role of two-site excitons in energy transfer to impurity centers in wide-band dielectrics and, second, explain experimental data on fast energy transport realized by two-site excitons.

Energy transfer from excitons to neutral impurity centers has been observed by many authors in dielectrics of various types. The character of the excitonic state, responsible for energy transfer, depends on the specific band structure of the dielectric crystal. Experimental data for wide-band dielectrics of the type considered provide evidence that energy transport is realized not by free excitons but by two-site excitonic polarons.

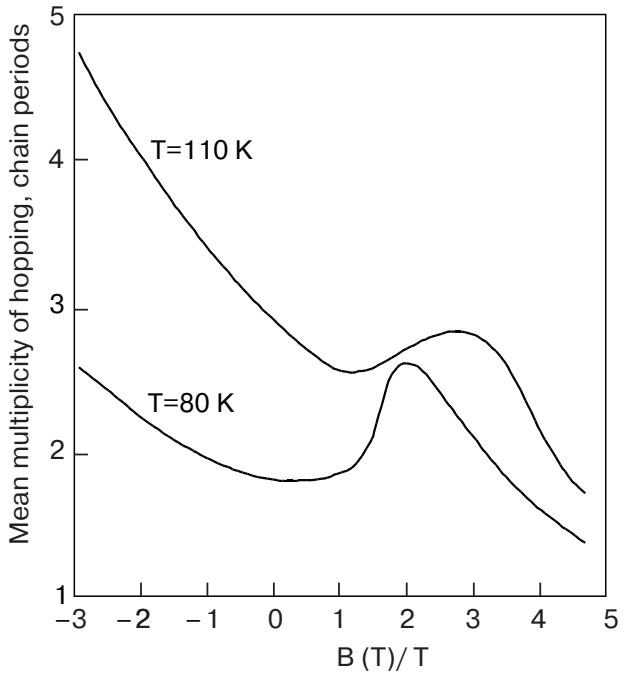

Fig. 7. Mean distance of hopping in units of the chain periods (hopping multiplicity), calculated at T = 80 K and 110 K.

5.1. Energy transport in alkali halide crystals.

The assumption of energy transfer by free excitons should be discarded for the following reason. Usually impurity levels lie below the bottom E_{bot} of the lowest exciton band. An exciton, before it can transfer its energy to such an impurity center, first must achieve E_{bot} via thermal relaxation. The quantum yield of creating excitons at the band bottom can be estimated from the quantum yield of the free-exciton luminescence, Y_{free} (in the crystals of the type considered, the radiative decay of excitons is possible only at the band bottom, where the exciton quasi-momentum goes to zero). For all the alkali halides examined [17], Y_{free} is of the order of 10^{-2}. Such a low quantum yield of the photoproduction of free excitons cannot provide efficient energy transfer to the impurity centers observed spectroscopically [14–16]. But even after an exciton has reached the band bottom, the transfer of its energy to an impurity atom must be preceded by localization in a shallow potential well near the impurity center; this is impeded by the rather small effective mass of a free exciton [9].

On the other hand, an efficient energy transfer to thallium impurity centers, present in a very low concentration of 10^{-6} to 10^{-5}, was observed in KI(Tl), RbI(Tl), and NaI(Tl) crystals under excitation below the bottom of the lowest excitonic band [14–16]. In this excitation energy region, two-site excitons are created with a high efficiency, but free excitons cannot be generated at all (which is confirmed by the zero quantum yield of free-exciton luminescence measured for pure KI, RbI, and NaI under excitation below E_{bot} [17]). Moreover, the efficiency of the energy transfer to the impurity did not grow as the excitation frequency was changed from a value below E_{bot} (where $Y_{free} = 0$) to any value lying inside the band (where $Y_{free} \sim 0.01$) [14].

Consider now the rate of energy transport realized by two-site excitons. The efficiency of the energy transfer to impurity centers can be characterized by the ratio Y_{imp}/Y_{host}, where Y_{imp} is the intensity of impurity luminescence and Y_{host} is the luminescence intensity of two-site excitons formed in the host crystal. The ratio Y_{imp}/Y_{host} was measured spectroscopically for the alkali halide crystals KI, RbI, and NaI weakly doped with thallium [14–16]. According to Refs. 14–16, efficient energy transfer to the impurity ($Y_{imp}/Y_{host} \approx 1$) at T = 5 K is achieved for KI(Tl), RbI(Tl), and NaI(Tl) at the concentrations n = = $1.5 \cdot 10^{16}$, $3 \cdot 10^{16}$, and $5 \cdot 10^{17}$ cm^{-3}, respectively. Let us show that the coherent directional motion of self-trapped excitons with the velocity V, investigated in Sec. 3, provides such an efficient energy transfer to the impurity, described by the relation

$$Y_{\text{imp}} / Y_{\text{host}} \approx V t \sigma\, n \sim 1. \qquad (16)$$

Here $t \approx 1$ ns stands for the vibrational relaxation time and σ is the cross section of the exciton localization near an impurity ion; the velocity V of the directional motion of two-site self-trapped excitons is taken equal to the longitudinal sound velocity in the crystal, near $2 \cdot 10^5$ cm/s.

The value of σ is determined by the interaction of an exciton with an impurity ion, described (in atomic units) by the van der Waals potential

$$U(R) = -\alpha_{\text{imp}} \left\langle r^2 \right\rangle R^{-6}, \qquad (17)$$

where $\left\langle r^2 \right\rangle$ is the squared state radius of the site exciton, and α_{imp} stands for the positive difference between the polarizability of the impurity atom (molecule) and that of the substituted lattice atom [9]. A two-site exciton, moving along the anion chain, can be localized near an impurity atom lying at a distance R from the chain if $|U(R)| > T$. This gives the estimate (in atomic units):

$$\sigma = \pi R^2 \approx \pi \left(\frac{\alpha_{\text{imp}} \left\langle r^2 \right\rangle}{T} \right)^{1/3}. \qquad (18)$$

With realistic values of the parameters: $\left\langle r^2 \right\rangle = 150$, $\alpha_{\text{imp}} = 40$ [9,18] at T=5 K, the estimate (18) gives $\sigma = 2300$ a. u. $= 6.3 \cdot 10^{-14}$ cm^2. For KI(Tl), RbI(Tl), and NaI(Tl), the right-hand side of Eq. (16) takes on the values 0.4, 0.6 and 6, respectively. Thus, the fast energy transfer to impurity, observed in Refs. 14–16, is explained qualitatively by directional motion of two-site excitons. (In view of the rather weak dependence of the trapping cross section (18) on the parameters, their choice cannot influence this conclusion.)

Experiment shows [14–16] that the ratio $Y_{\text{imp}} / Y_{\text{host}}$ decreases rapidly with increasing temperature, especially above 30 K. The observed temperature dependence of $Y_{\text{imp}} / Y_{\text{host}}$ is too strong to be described by Eqs. (16) and (18) with a constant V and should be attributed mainly to the temperature destruction of the coherent directional regime of the two-site exciton motion (see Sec. 3).

5.2. Energy transport in rare-gas crystals

For rare-gas crystals, the free-exciton mechanism of energy transfer should be discarded in view of the following experimental fact. The quantum yield Y_{imp} of the luminescence of a very weak impurity sharply grows with an increase of the excitation photon energy E near the point E_g of the dielectric gap width [19, 20]. This energy dependence of Y_{imp} cannot mirror the E dependence of the free-exciton photoproduction efficiency, which is of opposite character (a photon with $E < E_g$ inevitably generates a free exciton, whereas an electron and hole, generated at $E > E_g$, do not necessarily recombine in the form of a free exciton [21,8]).

However, this feature of the excitation spectrum can be easily understood in terms of the vibrational spectrum of two-site excitons, assuming that they are responsible for the energy transfer to impurities [8,20]. Indeed, a photon with $E > E_g$ generates an electron–hole pair. The hole is very rapidly self-trapped, turning into a two-site molecular ion. The latter, after recombination with an electron, becomes a two-site exciton related to a high excited atomic state (close to the ionization level) with a very large state radius $\langle r \rangle$ [9]. Due to the large $\langle r \rangle$, this excited state is strongly attracted to impurity centers by its van der Waals potential (17). On the other hand, a two-site exciton, occupying a high vibrational level (extended to a narrow subband), is a very heavy band particle [7]; the large $\langle r \rangle$ in combination with a large effective mass provides a high probability for a two-site exciton to be localized near an impurity center even at a very low concentration of impurity. A two-site exciton, localized on a high vibrational level, remains pinned at the same impurity center during vibrational relaxation, after which the exciton energy is transferred to the impurity. Under such conditions, a fast directional motion of two-site excitons provides an extremely efficient energy transfer to impurities. Note that the high motion velocity of two-site excitons, derived in Sec. 3 within the classical approach with allowance for a non-pair exchange potential, does not contradict the large effective mass of the two-site exciton subbands derived quantum-mechanically within the approach of a pairwise exchange potential (this seeming contradiction was elucidated in Ref. 10).

Quite a different relaxation picture takes place when a photon with $E<E_g$ turns to a free exciton (such optical transitions are partly allowed in a real crystal with lattice defects [22]). The generated exciton persists in a free state during the relaxation through the upper part of the exciton band where the free and two-site states are not mixed [9]. Unlike a two-site exciton, which can be localized on any vibrational level near an impurity center, a free exciton cannot be trapped inside the band on a impurity level lying below the band bottom, since this electronic transition requires a too strong jump-wise heat release. Only in the lower part of the band the free exciton is mixed with two-site states [7] and can be localized near an impurity center; but the localization probability is low because of a comparably small state radius.

6. Qualitative comparison with experiment. Mobility of two-site holes

6.1. Rare-gas crystals

The mobility of two-site holes in rare-gas crystals was measured experimentally [13] in a vicinity of the triple point, where the structural perfection of the samples was high enough to make such measurements possible. Table 2 presents the temperature change of the mobility of self-trapped holes in rare-gas crystals measured in the temperature interval $T_1 < T < T_2$ [13]. Both the experimental values of mobility and its temperature behavior observed strongly contradict the law (1) with activation energy $U_{\text{act}} \approx \Delta \sim 1$ eV. The conventional equation (1) predicts a negligibly small mobility and its highly sharp dependence on T. The observed mobility is comparatively high and its temperature variation is found to be weak (and even practically absent for krypton). This can be agreed with (1) only by substituting a very small binding energy E_b [13]. These values of E_b (given in the next-to-last column of Table 2) strongly differ from the true binding energy estimated from spectroscopic data and given in the last column. (The spectroscopic estimate of E_b [1] is related to the corresponding two-site excitonic state; it turns into the self-trapped hole after ionization, which can only enhance the binding energy [9].)

As shown in Sec. 4, these contradictions are naturally eliminated by taking into account the intrinsic vibrational structure of two-site hole polarons. Figure 5 shows that, depending on the barrier height, the calculated mobility can either grow or diminish somewhat with increasing temperature. This inference, as well as the absolute values of the mobility obtained, are in a qualitative agreement with experimental data listed in Table 2.

6.2. Alkali-halide crystals

As was already mentioned in Sec. 1, the anion sublattice of an alkali-halide crystal has a spectrum of electronic excitations similar to that of the corresponding rare-gas crystal (the electronic configuration of the anion, e.g., I^- or Cl^-, is identical with that of the corresponding rare-gas atom Xe or Ar, respectively). The spectrum of electronic excitations of the cation (Na^+, K^+ etc.) sublattice lies much higher and cannot interfere with the spectrum of the anion sublattice. In particular, a stable self-trapped state of an anion hole has the form of a two-site quasi-molecule similar to that formed in rare-gas crystals.

However, as regards the manner of motion of self-trapped holes, alkali-halide crystals exhibit a distinction from rare-gas solids. As was mentioned in Sec. 2, lattice atoms, lying beyond the chain, to some degree hamper the motion of the chain atoms, so that the lattice surroundings of the chain heighten the barrier. In alkali-halide crystals, the effect of the lattice surroundings on the barrier depends on the separation, d_{AC}, of an anion from the nearest cation, or, more exactly, on the ratio of d_{AC} to the distance d_{AA} between adjacent anions within the chain. The barrier height grows with a decrease of the ratio d_{AC}/d_{AA} and, quite naturally, with an increase of the cation-to-anion size ratio.

Such an effect of the lattice surroundings on the barrier B is illustrated by Table 3, based on the experimental data of Ref. 2. The lowest barrier of about 0.1 eV was observed for the case of the largest anion I^- and the smallest cation Na^+. Although Cs^+ signifi-

Table 2

Brief summary of experimental data on the self-trapped hole mobility μ in rare-gas crystals measured in the temperature interval $T_1 < T < T_2$ near the triple point [13]. The next-to-last column gives the polaron binding energy E_b found in Ref. 13 by fitting Eq. (1) with the experimental dependence $\mu = \mu(T)$; the last column presents an independent realistic estimate of E_b from spectroscopic data [1]. Note that the conventional theory, making no allowance for the intrinsic structure of a self-trapped hole [3–6], cannot explain a weak temperature dependence of μ, drastically contradicting to Eq. (1) with the true binding energy $E_b \sim 1$ eV.

Crystal	T_1	T_2	$\mu(T_1)$	$\mu(T_2)$	E_b, eV	
	K		in units 0.01 $cm^2 \cdot V^{-1} \cdot s^{-1}$		from $\mu(T)$ [13]	spectroscopically
Ne	18	25	0.2	1.05	0.024	>1.9
Ar	71	83	1.2	2.3	0.07	>1.2
Kr	84	113	4.0 ± 0.5	4.0 ± 0.5	0.04	>0.9
Xe	110	160	3.2	1.8	0.005 to 0.02	>0.7

cantly exceeds Na^+ in size, the barrier remains almost the same for CsI due to a greater ratio $d_{AC}/d_{AA} = 3^{1/2}/2$ for the body-centered cell (for a rare-gas crystal, the corresponding ratio equals unity). The barrier gradually grows, due to a decrease of the anion size, in the sequence CsI – CsBr – CsCl and rises sharply (despite a decrease of the cation size) when changing to the KCl crystal, with a smaller d_{AC}/d_{AA} ratio. The difference in B between KCl and NaI manifests itself in a sharp difference in mobility (10^{-3} $cm^2 \cdot s^{-1} \cdot V^{-1}$ for NaI and 10^{-10} $cm^2 \cdot s^{-1} \cdot V^{-1}$ for KCl) [2].

Table 3

Height of the barrier for translational motion B and axis reorientation B_{reor} of two-site self-trapped holes in alkali halides according to the experimental data of Ref. 2. d_{AC} is the separation of an anion from the nearest cation and d_{AA} is that between adjacent anions.

Crystal	NaI	CsI	CsBr	CsCl	KCl
d_{AC}/d_{AA}	0.707	0.866	0.866	0.866	0.707
B, eV	0.1	0.13	0.20	0.24	0.57
B_{reor}, eV	0.18	0.20	0.37	–	0.54

Along with this, Table 3 contains data related to the reorientation of the hole axis, i.e., changing the hole polarization direction [2]. These data provide evidence for a one-dimensional character of the two-site hole motion (stated in Sec. 1). The motion of a hole along the anion chain is accompanied by conservation of its polarization direction (parallel to the chain). A hole changes its motion direction (escaping to another chain intersecting the former one) simultaneously with changing the polarization direction. So, the distance (in units of the chain periods), traveled by a hole along the chain before hopping to another chain, can be estimated as

$$\frac{P_{transl}}{P_{reor}} \sim \exp\left(\frac{B_{reor} - B}{T}\right), \qquad (19)$$

where P_{transl} and B denote the rate and barrier height for the hole translational motion; P_{reor} and B_{reor} are those for the hole axis reorientation.

As is seen from Table 3, B_{reor} exceeds B by about 1000 K which provides a predominant motion of a hole within the same chain with infrequent hops between different chains. The difference $B_{reor} - B$ is negative only for KCl that drops out of the developed scheme, being nearer to the conventional notion; but even for KCl, P_{transl} was found to exceed P_{reor} at least by an order of magnitude [2]. In Ref. 2 a general conclusion for alkali halides was reached that the number of translational hops of a two-site hole greatly exceeds the number of reorientation hops.

Acknowledgement

The author is thankful to A.N. Ogurtsov and E.V. Savchenko for helpful discussions.

This work was carried out within the project DFG No. 436 UKR 113/55/0.

1. I.Ya. Fugol', *Adv. Phys.* **27,** 1 (1978).
2. E.D. Aluker, D.Yu. Lusis, and S.A. Chernov, *Electronic Excitations and Radioluminescence of Alkali Halide Crystals*, Riga Zinatne, Latvia (1979) (in Russian).
3. T. Holstein, *Ann. Phys.* N.Y. **8,** 343 (1959).
4. D. Emin and T. Holstein, *Ann. Phys* N.Y. **53**, 439 (1969).
5. D. Emin, *Phys. Rev.* **B3,** 1321 (1971).
6. D. Emin, *Phys. Rev.* **B4**, 3639 (1971).
7. A.M. Ratner, *J. Luminesc.*, **81**, 271 (1999).
8. A.M. Ratner, *Phys. Lett.* **A265**, 411 (2000).
9. A.M. Ratner, *Phys. Rep.* **269,** 197 (1996).
10. A.M. Ratner, *Phys. Lett.* **A291**, 165 (2001).
11. A.M. Ratner, *Phys. Lett.* **A298**, 422 (2002).
12. K.S. Song, *Canadian J. Phys.* **49**, 26 (1971).
13. P.G. Le Comber, R.J. Loveland, and W.E. Spear, *Phys. Rev.* **B11**, 3124 (1975).
14. M. Tomura, O. Fujii, and H. Nishimura, *J. Phys. Soc. Jpn.* **41**, 194 (1976).
15. H. Nishimura, T. Kubota, and M. Tomura, *J. Phys. Soc. Jpn.* **42,** 175 (1977).
16. H. Nishimura and M. Tomura, *J. Phys. Soc. Jpn.* **39**, 390 (1976).
17. H. Nishimura and T. Yamano, *J. Phys. Soc. Jpn.* **51**, 2947 (1982).
18. P. Gombas, *Theorie und Losungsmethoden des Mehrteilchenproblems der Wellenmechanik*. Basel, (1950).
19. M. Haevecker, M. Runne, and G. Zimmerer, *Electron Spectr. Related Phenomena* **79**, 103 (1996).
20. A.N. Ogurtsov, A.M. Ratner, E.V. Savchenko, V. Kisand, and S. Vielhauer, *J. Phys.: Condens. Matter* **12,** 2769 (2000).
21. D. Varding, I. Reimand, and G. Zimmerer, *Phys. Status. Solidi*. **B185**, 301 (1994).
22. A.M. Ratner, *Phys. Lett.* **A269**, 245 (2000).